Smart Foldamers

DOI: 10.1002/anie.201307378

Control over Unfolding Pathways by Localizing Photoisomerization Events within Heterosequence Oligoazobenzene Foldamers**

*Zhilin Yu and Stefan Hecht**

In the field of foldamers,[1] the dynamics of the helix–coil transition are of particular importance for molecular recognition processes, such as guest binding,[2] as well as for the formation of intertwined aggregates (double helices).[3] In both processes, the unfolding/refolding pathway that proceeds either from the termini to the helix core ("outside in") or vice versa ("inside out") plays a crucial role. During our investigations of photoswitchable foldamers,[4,5] we found that the location of the light-responsive azobenzene units within the backbone governs their ability to photoisomerize and hence to locally induce helix unfolding. This position-dependent photoisomerization behavior[4d,e] should in principle allow for the desired control over the unfolding/refolding pathway if the photoexcitation can be exclusively localized at the specific photoisomerization site, either at the helix terminus or the core. Inspired by the ability of natural light-harvesting systems to funnel excitation energy to a specific site,[6] we sought to incorporate additional azobenzene units, which act as energy traps, into our established oligoazobenzene foldamer scaffold. Upon global (broad band) excitation, such gradient architectures that incorporate the traps either at the termini or at the core should allow control over the unfolding pathway to occur outside in or inside out, respectively. Herein, we report the design and synthesis of a pair of heterosequence foldamers that are composed of two different azobenzene photochromes (donor and acceptor) as well as spectator *meta*-phenylene units, and the investigation of their light-induced unfolding processes that are governed by the localization of the photoisomerization event.

In this study, 4,4′-dimethoxy-substituted azobenzene (DMAB) units were used because they display a bathochromic shift of their $\pi\rightarrow\pi^*$ absorption band by 30 nm relative to that of the parent azobenzene repeat units,[4a,b] which renders them the most red-shifted chromophore in the foldamer and hence the global energy acceptor sites, or traps.[6] The cross-conjugated *meta* linkages ensure decoupling of the individual phenylene/tolane, azobenzene, and DMAB chromophore repeat units. The DMAB unit does not only localize the excitation, but also exhibits a photoisomerization efficiency that is superior to that of the parent azobenzene photochrome.[7]

To test the influence of localizing the photoisomerization event on the unfolding pathway, the DMAB unit was incorporated either at the termini or at the core of the parent foldamer backbone.[4e] Therefore, the oligomers $\mathbf{14_{3\text{-}2}}$ and $\mathbf{14_{4\text{-}1}}$ were synthesized and compared to the parent foldamer $\mathbf{14_5}$, which solely contains identical azobenzene repeat units (Figure 1, left). In all three foldamers, individual azobenzene photochromes are connected through *meta*-phenylene units that enforce an arrangement of two azobenzene units per helix turn, which results in cofacial π–π stacking of the azobenzenes along the helix axis (Figure 1, right).[4e] The introduction of polar oligo(ethylene glycol) side chains provides the solvophobic driving force for folding in a polar medium; in addition, their chiral centers induce helicity, which aids the conformational analysis by circular dichroism (CD) spectroscopy.[4,8] The syntheses of the oligomers were carried out by iterative routes that mostly relied on statistical palladium-catalyzed Sonogashira–Hagihara coupling reactions[9] and employed suitable brominated azobenzene and DMAB units as well as 3,5-diiodobenzoate[10] fragments (see the Supporting Information, Scheme S1 and S2).[11] The synthesized target compounds $\mathbf{14_{4\text{-}1}}$ and $\mathbf{14_{3\text{-}2}}$ were fully characterized with regard to their chemical structure and purity by various techniques, including ^{1}H NMR spectroscopy, MALDI-TOF mass spectrometry, and gel permeation chromatography (GPC).[11]

The conformations of both oligomers as their *all-E* isomers were determined in a solvent titration experiment in which unfolding was induced by increasing the chloroform content of an acetonitrile solution while monitoring UV/Vis absorption[12] and recording CD[8] spectra. In the corresponding UV/Vis spectra (Figure S5),[11] the appearance of a new absorption band at approximately 310 nm upon addition of chloroform is indicative of the local *cisoid*→*transoid* conformational transition. Concomitantly, in the CD spectra (Figure S6),[11] the initially observed Cotton effect decreases until it completely vanishes in neat chloroform, which independently confirms helix unfolding.[4d] Both of these results imply that the oligomer only adopts a stable helical conformation in the polar medium acetonitrile. From these denaturation experiments, the helix stabilization energies of the oligomers in neat acetonitrile [ΔG (CH_3CN)] were obtained by plotting the ratio between the absorption

[*] Dr. Z. Yu,[+] Prof. Dr. S. Hecht
Department of Chemistry, Humboldt-Universität zu Berlin
Brook-Taylor-Strasse 2, 12489 Berlin (Germany)
E-mail: sh@chemie.hu-berlin.de

[+] Current address: Institute for BioNanotechnology in Medicine
Northwestern University
Chicago, IL (USA)

[**] We thank Dr. Steffen Weidner (BAM) for MALDI-TOF MS characterization. Generous support by the German Research Foundation (DFG; SFB 765) and the European Research Council (ERC-2012-STG_308117; "Light4Function") is gratefully acknowledged. BASF AG, Bayer Industry Services, and Sasol Germany are thanked for generous donations of chemicals.

Supporting information for this article, including experimental and characterization data, is available on the WWW under http://dx.doi.org/10.1002/anie.201307378.

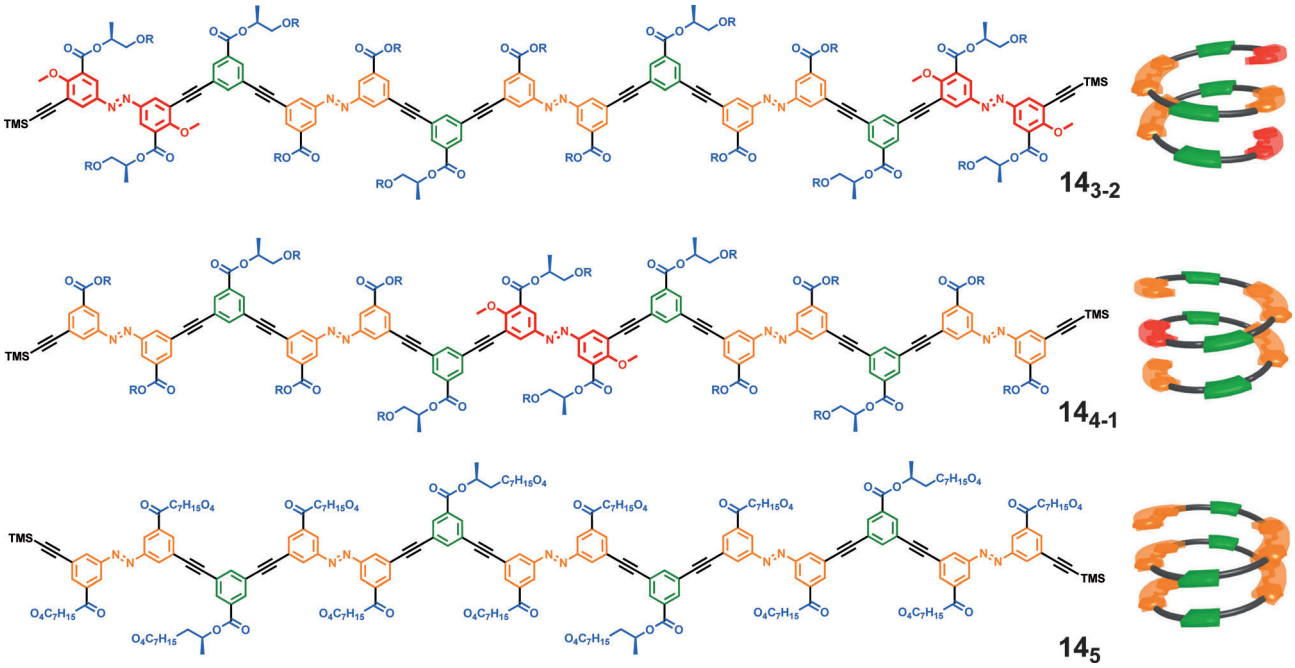

Figure 1. Investigated heterosequence foldamers $\mathbf{14_{3-2}}$ and $\mathbf{14_{4-1}}$ as well as reference foldamer[4e] $\mathbf{14_5}$: Chemical structures (left) and schematic representations of their helically folded structure (right). The foldamers are shown as their *all-E* isomers with R = $(CH_2CH_2O)_3CH_3$) and their individual repeat units have been marked in specific colors: DMAB (red), azobenzene (orange), and *meta*-phenylene (green). In the used nomenclature, the number 14 denotes the overall number of aromatic benzene units, while the subscripts denote the number of regular azobenzene units followed by the number of incorporated DMAB moieties. TMS = trimethylsilyl.

intensities of the *transoid* and *cisoid* conformers as a function of solvent composition (Figure S7).[11–13] Foldamer $\mathbf{14_{3-2}}$, which bears DMAB units at its termini, exhibits a slightly lower helix stabilization energy than foldamer $\mathbf{14_{4-1}}$, which incorporates the DMAB unit in the core (Table 1). This difference in stability is not related to the type of π–π stacking interactions as observed previously[4e] as they remain the same in both foldamer helices; instead, we assume a slightly weaker contact in the case of the more electron-rich terminal DMAB units.[14] Interestingly, the twist sense bias of these two foldamers is opposite to each other; foldamer $\mathbf{14_{3-2}}$ shows a negative Cotton effect, whereas foldamer $\mathbf{14_{4-1}}$ displays a positive Cotton effect in the CD spectra, similarly to $\mathbf{14_5}$ and in fact all other previously investigated tetradecamers ($\mathbf{14_4}$ and $\mathbf{14_7}$).[4e] The opposite handedness observed for foldamer $\mathbf{14_{3-2}}$ most likely originates from the placement of most of the chiral side chains at the termini (attached to the terminal DMAB units) as the specific location of chiral side chains in the backbone likely dictates the twist sense of a helix.[15] These different interactions between the side chains might also explain the observed slightly different helix stabilities.

Table 1: Folding and photoswitching parameters of foldamers $\mathbf{14_{3-2}}$ and $\mathbf{14_{4-1}}$ and reference foldamer $\mathbf{14_5}$ in acetonitrile at 25 °C.

Parameter		$\mathbf{14_{3-2}}$	$\mathbf{14_5}$	$\mathbf{14_{4-1}}$
ΔG (CH_3CN)[a] [kcal mol^{-1}]		−2.68 ± 0.18	−3.38 ± 0.20	−2.95 ± 00.20
k (*unfold*)[b] [10^2 s^{-1}]		3.84 ± 0.09	1.21 ± 0.02	3.62 ± 00.09
Z content at PSS [%][c]	Z_{term}	62.5 ± 0.5 %	←45.5 ± 0.6 %→	39.6 ± 0.4 %
	Z_{core}	22.3 ± 0.3 %[d]	←31.3 ± 0.3 %→	37.5 ± 0.5 %[d]
	Z_{av}	38.4 ± 0.6 %	37.0 ± 0.6 %	33.6 ± 0.6 %

[a] Derived from UV/Vis spectral changes. [b] Derived from CD spectral changes. [c] Determined by ^{1}H NMR spectroscopy (for terminal, internal, and core azobenzenes as shown in Figure S12, 13; Z_{av} = mathematical average). [d] The internal azobenzene could not be distinguished from the core azobenzene; hence, their average value is given.

After confirming the helical backbone conformation of $\mathbf{14_{3-2}}$ and $\mathbf{14_{4-1}}$ in their *all-E* configuration in acetonitrile, these solutions were subjected to UV irradiation, which induced $E \rightarrow Z$ photoisomerization of the embedded azobenzene units to trigger helix unfolding. Upon exposure to 358 nm light, a decreasing π→π* absorption band at 287 nm and a slightly increasing n→π* absorption band at approximately 440 nm were observed for both foldamers (Figure 2, top; Figure S9),[11] indicating the occurrence of the photoinduced $E \rightarrow Z$ isomerization in azobenzene photochromes.[7b] Whereas UV/Vis spectra provide information about the local photochemistry, the CD spectra allow for evaluation of the overall chain conformation; indeed, the significant decrease of the Cotton effect (Figure 2, bottom) indicated an efficient helix–coil transition, or unfolding, as a consequence of $E \rightarrow Z$ photoisomerization.

To gain insight into the localization of the individual photoswitching event(s), ^{1}H NMR spectroscopy was used and greatly facilitated by different substitution patterns of the azobenzene repeat units, which allowed their spectral separation and unambiguous identification (Figure S12 and S13).[11] At the photostationary state (PSS), NMR analysis

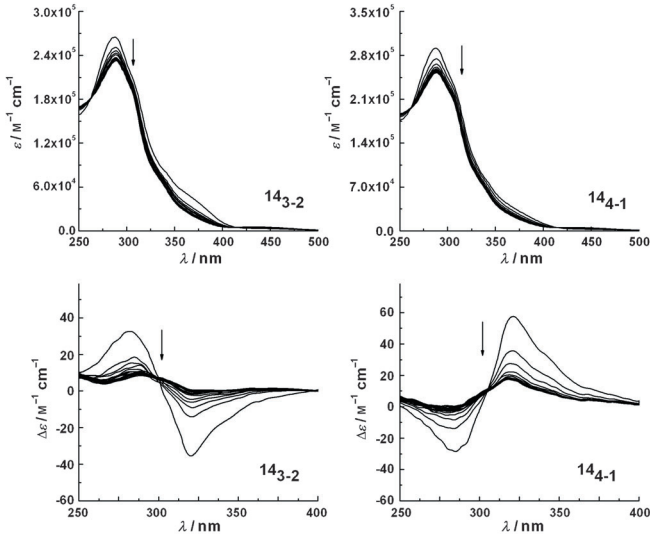

Figure 2. UV/Vis absorption (top) and CD (bottom) spectra indicate photochemical $E \rightarrow Z$ isomerization of oligomers $\mathbf{14_{3\text{-}2}}$ and $\mathbf{14_{4\text{-}1}}$ during irradiation ($\lambda_{irr} = 358$ nm) in CH_3CN at 25 °C.

provided an average distribution of $E \rightarrow Z$ photoisomerization throughout the backbone, which is expressed as the Z content (Table 1). In comparison with the parent foldamer $\mathbf{14_5}$,[4e] the occurrence of $E \rightarrow Z$ photoisomerization is specifically enhanced in the positions occupied by DMAB units (Table 1). The relative increase of the Z content at the terminal and central DMAB positions amounts to 37 % and 20 % in $\mathbf{14_{3\text{-}2}}$ and $\mathbf{14_{4\text{-}1}}$, respectively, relative to foldamer $\mathbf{14_5}$ (Table 1; see also Figure S15).[11]

These findings indicate that $E \rightarrow Z$ photoisomerization preferably occurs at the DMAB sites, which implies that the localization of individual isomerization events at the desired positions within these heterosequence foldamers has been improved. In conjunction with the improvement of the Z content of the DMAB units, the Z content of the parent azobenzene units is decreasing.

The enhanced localization of $E \rightarrow Z$ photoisomerization events can in principle be attributed to an intrinsically higher photoreactivity of the DMAB units and/or an efficient mechanism to funnel the excitation energy to the DMAB sites. The first option results from a combination of a higher extinction coefficient and a higher quantum yield of the DMAB photochrome upon 358 nm excitation. However, exposure to 320 nm irradiation, where the parent azobenzene absorbs more strongly, showed the same tendency of localizing $E \rightarrow Z$ photoisomerization at the DMAB sites (Table S2),[11] which indicates that the latter option might be the operating mechanism. In this alternative or additional scenario, an efficient energy-transfer cascade that involves various absorbing chromophores,[16] such as the tolane and parent azobenzene donors and the DMAB acceptor(s), would cause localization of excitation at the DMAB sites, which is followed by their isomerization. Such an energy-transfer mechanism would largely benefit from a chromophore arrangement that allows for their strong coupling, for example, in a compact helix conformation with a small pitch leading to π–π stacking. To investigate the effect of the chain conformation on localizing the $E \rightarrow Z$ photoisomerization events, the Z content of azobenzene units was also analyzed at the PSS in chloroform; in this solvent, the backbone adopts a random-coil conformation (Table S3).[11] Whereas in $\mathbf{14_5}$ an almost identical Z content was observed at different positions, a higher Z content of DMAB units remained in foldamers $\mathbf{14_{3\text{-}2}}$ and $\mathbf{14_{4\text{-}1}}$. However, the Z content at the positions occupied by the DMAB moieties was revealed to be significantly greater in acetonitrile than in chloroform (Figure S15).[11] This important finding of improved localization of the $E \rightarrow Z$ photoisomerization events demonstrates the superior performance of the helix structure in the energy-transfer process. In light of these results, and considering the decrease of the Z content of the parent azobenzene units relative to foldamer $\mathbf{14_5}$ (Table 1), we speculate that energy transfer between the two different azobenzene units (and possibly the tolane units)[17] is largely responsible for the observed preferential DMAB isomerization. The better inherent switching ability of the DMAB unit[7] certainly plays an additional role. Further investigations of the energy transfer pathway require the use of time-resolved spectroscopic studies, which suffer from fluorescence quenching for helical conformations and strong solvent background signals for random-coil structures.[7,18]

Although a detailed microscopic insight into the unfolding dynamics is currently not available, monitoring the changes in the UV/Vis and CD spectra during irradiation provides important kinetic information. Analysis of the UV/Vis spectral evolution is not conclusive (Figure S10 and Table S1)[11] as the spectra are the result of superimposed photoisomerization events in all azobenzene subunits of every folded and unfolded species present in solution, and hence neither unfolding rates nor rates of the initial $E \rightarrow Z$ photoisomerization can be deduced. However, CD spectroscopy proved to be particularly useful in this case as it is only sensitive to conformational changes and therefore can be used as a direct measure of the helix–coil transition.[4d] Analysis of the decay of the CD signal over time (Figure S11)[11] provided the unfolding rates, which showed that foldamer $\mathbf{14_{3\text{-}2}}$ isomerizes more quickly than $\mathbf{14_{4\text{-}1}}$ (Table 1). Furthermore, both foldamers unfolded about three times faster than the parent homoazobenzene foldamer $\mathbf{14_5}$. The CD-derived rates describe the overall unfolding process, which includes both initial $E \rightarrow Z$ photoisomerization and subsequent helix→coil transition, which are strongly coupled events.

Shifting the initial $E \rightarrow Z$ photoisomerization events to either terminal or core DMAB sites results in two different unfolding pathways, namely outside in or inside out, which are associated with different kinetic barriers and rates. In foldamers that contain identical azobenzene units, denaturation of the helical structure predominantly arises from terminal isomerization processes as described previously;[4c] in foldamers $\mathbf{14_{3\text{-}2}}$ and $\mathbf{14_{4\text{-}1}}$, however, the location of the DMAB units has a significant impact on their unfolding processes (Scheme 1). Most notably, in $\mathbf{14_{3\text{-}2}}$, terminal isomerization processes occur much more frequently than central isomerization, and therefore, unfolding should mainly proceed through an outside–in pathway. In its foldamer counter-

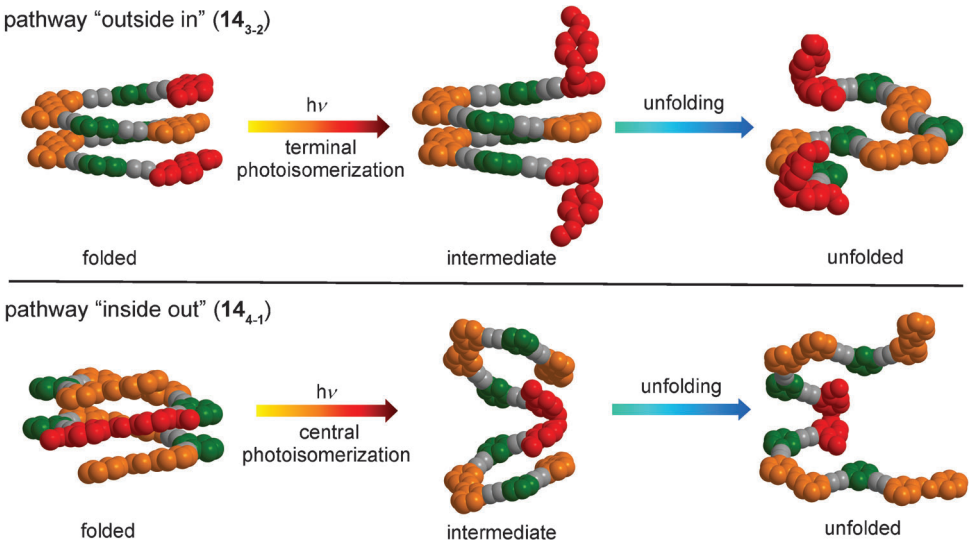

Scheme 1. Two competing unfolding pathways that are triggered by the localization of photoisomerization events at the DMAB sites.

part $\mathbf{14_{4\text{-}1}}$, core isomerization, which clearly is a disfavored process in $\mathbf{14_5}$, becomes as important as the terminal isomerization processes, which enhances the population of foldamers that follow the inside–out unfolding route. The kinetic data suggest that this inside–out unfolding pathway is associated with a slightly higher barrier, which we attribute to π–π contacts that are more enhanced at the core DMAB site than at the terminal DMAB sites, which results in a lower quantum yield.

In summary, we have designed two distinct photoswitchable foldamers; their isomerization events can be specifically localized in desired positions by the site-specific incorporation of a suitable azobenzene unit as the energy acceptor. Based on the localization of the unfolding trigger, it is possible to modulate the partitioning between the two competing unfolding pathways. Attempts to investigate the underlying mechanism for the enhanced localization of the photoisomerization events that are particularly concerned with unraveling the internal energy transfer processes are currently underway. Furthermore, the unfolding dynamics of these systems will be investigated using advanced theoretical[19] and experimental approaches, in particular time-resolved vibrational spectroscopy.[20] The strategy outlined herein should prove viable for the design of sophisticated architectures based on photoswitchable foldamer hosts for remote-controlled dynamic recognition[2,3] and catalysis,[21] as well as for advanced optomechanical systems.[22] Future target structures will aim at improving control over the unfolding pathway by exclusive localization of the photoisomerization site and at lowering the unfolding barriers, in particular for the "inside out" case. Control over the unfolding pathway may also trigger the mimicry of natural systems involved in biological, mostly nucleic acid, helix transformations, such as helicases and topoisomerases.

Received: August 22, 2013
Revised: October 12, 2013
Published online: November 19, 2013

Keywords: azobenzenes · circular dichroism · energy transfer · foldamers · photochromism

[1] a) D. J. Hill, M. J. Mio, R. B. Prince, T. S. Hughes, J. S. Moore, *Chem. Rev.* **2001**, *101*, 3893–4012; b) *Foldamers: Structure, Properties, and Applications* (Eds.: S. Hecht, I. Huc), Wiley-VCH, Weinheim, **2007**; c) G. Guichard, I. Huc, *Chem. Commun.* **2011**, *47*, 5933–5941.

[2] For a review, see: a) J. Becerril, J. M. Rodriguez, I. Saraogi, A. D. Hamilton in *Foldamers: Structure, Properties, and Applications* (Eds.: S. Hecht, I. Huc), Wiley-VCH, Weinheim, **2007**, chap. 7, p. 195; for prominent examples involving foldamer hosts, see: b) A. Tanatani, M. J. Mio, J. S. Moore, *J. Am. Chem. Soc.* **2001**, *123*, 1792–1793; c) J.-L. Hou, X.-B. Shao, G.-J. Chen, Y.-X. Zhou, X.-K. Jiang, Z.-T. Li, *J. Am. Chem. Soc.* **2004**, *126*, 12386–12394; d) M. Inouye, M. Waki, H. Abe, *J. Am. Chem. Soc.* **2004**, *126*, 2022–2027.

[3] For important examples, see: a) V. Berl, I. Huc, R. Khoury, M. Krische, J.-M. Lehn, *Nature* **2000**, *407*, 720–723; b) Y. Tanaka, H. Katagiri, Y. Furusho, E. Yashima, *Angew. Chem.* **2005**, *117*, 3935–3938; *Angew. Chem. Int. Ed.* **2005**, *44*, 3867–3870.

[4] a) A. Khan, C. Kaiser, S. Hecht, *Angew. Chem.* **2006**, *118*, 1912–1915; *Angew. Chem. Int. Ed.* **2006**, *45*, 1878–1881; b) A. Khan, S. Hecht, *Chem. Eur. J.* **2006**, *12*, 4764–4774; c) Z. Yu, S. Hecht, *Angew. Chem.* **2011**, *123*, 1678–1681; *Angew. Chem. Int. Ed.* **2011**, *50*, 1640–1643; d) Z. Yu, S. Hecht, *Chem. Eur. J.* **2012**, *18*, 10519–10524; e) Z. Yu, S, Weidner, T. Risse, S. Hecht, *Chem. Sci.* **2013**, *4*, 4156–4167; f) S. R. Domingos, S. J. Roeters, S. Amirjalayer, Z. Yu, S. Hecht, S. Woutersen, *Phys. Chem. Chem. Phys.* **2013**, *15*, 17263–17267.

[5] a) C. Tie, J. C. Gallucci, J. R. Parquette, *J. Am. Chem. Soc.* **2006**, *128*, 1162–1171; b) E. D. King, P. Tao, T. T. Sanan, C. M. Hadad, J. R. Parquette, *Org. Lett.* **2008**, *10*, 1671–1674; c) Y. Hua, A. H. Flood, *J. Am. Chem. Soc.* **2010**, *132*, 12838–12840; d) Y. Wang, F. Bie, H. Jiang, *Org. Lett.* **2010**, *12*, 3630–3633; e) H. Sogawa, M. Shiotsuki, H. Matsuoka, F. Sanda, *Macromolecules* **2011**, *44*, 3338–3345.

[6] For a review on light-harvesting systems, see: G. D. Scholes, G. R. Fleming, A. Olaya-Castro, R. van Grondelle, *Nat. Chem.* **2011**, *3*, 763–774.

[7] Upon $\pi\rightarrow\pi^*$ excitation, the parent azobenzene exhibits a quantum yield for $E\rightarrow Z$ photoisomerization of $\Phi = 0.11$ in *n*-hexane (see Ref. [7b]), whereas DMAB exhibits a quantum yield of $\Phi = 0.36$ in toluene; see: a) J. Olmsted III, J. Lawrence, G. G. Yee, *Solar Energy* **1983**, *30*, 271–274; for a recent overview of azobenzene photochemistry and photophysics, see: b) H. M. Dhammika Bandara, S. C. Burdette, *Chem. Soc. Rev.* **2012**, *41*, 1809–1825.

[8] a) R. B. Prince, L. Brunsveld, E. W. Meijer, J. S. Moore, *Angew. Chem.* **2000**, *112*, 234–236; *Angew. Chem. Int. Ed.* **2000**, *39*, 228–230; b) R. B. Prince, J. S. Moore, L. Brunsveld, E. W. Meijer, *Chem. Eur. J.* **2001**, *7*, 4150–4154.

[9] "Cross-Coupling Reactions to sp-C-atoms": K. Sonogashira in *Metal Catalyzed Cross-Coupling Reactions* (Eds.: F. Diederich, P. J. Stang), Wiley-VCH, Weinheim, **1998**, chap. 5.

[10] During palladium-catalyzed coupling reactions at temperatures that exceed 60 °C (necessary to couple less reactive methoxy-substituted building blocks with arylbromides) decomposition occurs.
[11] See the Supporting Information.
[12] a) J. C. Nelson, J. G. Saven, J. S. Moore, P. G. Wolynes, *Science* **1997**, *277*, 1793 – 1796; b) R. B. Prince, J. G. Saven, P. G. Wolynes, J. S. Moore, *J. Am. Chem. Soc.* **1999**, *121*, 3114 – 3121.
[13] B. H. Zimm, J. K. Bragg, *J. Chem. Phys.* **1959**, *31*, 526 – 535.
[14] For a related study on phenylene ethynylene foldamers, see: a) S. Lahiri, J. L. Thompson, J. S. Moore, *J. Am. Chem. Soc.* **2000**, *122*, 11315 – 11319; for reviews on π – π stacking, see: b) C. A. Hunter, K. R. Lawson, J. Perkins, C. J. Urch, *J. Chem. Soc. Perkin Trans. 2* **2001**, 651 – 669; c) E. A. Meyer, R. K. Castellano, F. Diederich, *Angew. Chem.* **2003**, *115*, 1244 – 1287; *Angew. Chem. Int. Ed.* **2003**, *42*, 1210 – 1250.
[15] For an early example of inducing CD with a terminally placed chiral side chain, see: H. Jiang, C. Dolain, J.-M. Léger, H. Gornitzka, I. Huc, *J. Am. Chem. Soc.* **2004**, *126*, 1034 – 1035.
[16] For representative examples of such energy-gradient architectures, see: a) C. Devadoss, P. Bharathi, J. S. Moore, *J. Am. Chem. Soc.* **1996**, *118*, 9635 – 9644; b) T. Weil, E. Reuther, K. Müllen, *Angew. Chem.* **2002**, *114*, 1980 – 1984; *Angew. Chem. Int. Ed.* **2002**, *41*, 1900 – 1904; c) W. R. Dichtel, S. Hecht, J. M. J. Fréchet, *Org. Lett.* **2005**, *7*, 4451 – 4454.
[17] Unpublished results in collaboration with the group of J. Wachtveitl.
[18] Attempts to utilize time-resolved fluorescence spectroscopy in acetonitrile or dichloromethane/chloroform solutions that were carried out in the group of G. D. Scholes, University of Toronto, were not successful.
[19] M. Böckmann, S. Braun, N. L. Doltsinis, D. Marx, *J. Chem. Phys.* **2013**, *139*, 084108.
[20] M. R. Panman, P. Bodis, D. J. Shaw, B. H. Bakker, A. C. Newton, E. R. Kay, A. M. Brouwer, W. J. Buma, D. A. Leigh, S. Woutersen, *Science* **2010**, *328*, 1255 – 1258.
[21] S. F. M. van Dongen, J. Clerx, K. Nogaard, T. G. Bloemberg, J. J. L. M. Cornelissen, M. A. Trakselis, S. W. Nelson, S. J. Benkovic, A. E. Rowan, R. J. M. Nolte, *Nat. Chem.* **2013**, *5*, 945 – 951.
[22] D. Bléger, Z. Yu, S. Hecht, *Chem. Commun.* **2011**, *47*, 12260 – 12266.

